Journal of Power Sources 195 (2010) 1370–1374

Contents lists available at ScienceDirect

Journal of Power Sources

journal homepage: www.elsevier.com/locate/jpowsour

Short communication

Carbon-supported manganese oxide nanocatalysts for rechargeable lithium–air batteries

H. Cheng*, K. Scott

School of Chemical Engineering & Advanced Materials, Newcastle University, Newcastle Upon Tyne NE1 7RU, UK

ARTICLE INFO

Article history:
Received 8 July 2009
Received in revised form 7 September 2009
Accepted 10 September 2009
Available online 20 September 2009

Keywords:
Rechargeable lithium–air battery
Manganese oxide nanocatalysts
Air electrode
Carbon
Discharge capacity
Cycle ability

ABSTRACT

Manganese oxide based catalysts were synthesised in the form of nano-particles using a redox reaction of $MnSO_4$ and $KMnO_4$, housed into the pores of a carbon matrix and followed by a thermal treatment. Particle sizes of the manganese oxide nanocatalysts were around 50 nm, based on the tunnelling electron microscope measurement. They were uniformly distributed in the carbon matrix, which contributed to an improved electrical connection among the catalyst and current collectors. The charge/discharge tests using this material as the cathode material in a rechargeable lithium–air battery showed high discharge capacities up to 4750 mAh (g carbon)$^{-1}$. The cycle ability of the composite electrode was superior to those of the commercial electrolytic manganese dioxide electrodes.

1. Introduction

There is growing interest in hybrid electric vehicles requiring smaller and lighter weight batteries to meet today's energy and environmental challenges. Rechargeable Li batteries have been considered as serious and realistic contenders for such applications [1–5]. Unfortunately, the energy density of current rechargeable lithium batteries was limited by the positive electrode $LiCoO_2$ (130 mAh g^{-1}). A revolutionary advance from graphite–$LiCoO_2$ batteries to Li–air counterparts is that these batteries allow lithium ions and electron in the cell to react with oxygen from air external to the battery as needed. The most striking feature of lithium-metal–air batteries is that they can in theory store a tremendous amount of energy. In terms of specific capacity, for lithium metal alone 1.3×10^4 Wh kg^{-1}; for the lithium and air, 1.1×10^4 Wh kg^{-1}, not including the weight of oxygen, and 5.2×10^3 Wh kg^{-1} including the weight of oxygen, thus increasing storage capacities and significantly reducing cost [1–5]. Hence capacities are 10-times as much as current high-performance lithium-ion batteries and more than any other class of energy-storage devices. This step-change in capacity could pave the way for a new generation of electric cars, mobile phones and laptops.

Lithium–air batteries are compact, lightweight and cost-effective because they adopt cheap and light materials that use oxygen drawn from the air during discharge, replacing expensive chemical constituents used in current rechargeable batteries.

The lithium–air battery also has the potential to give a major boost to the renewable energy industry. The battery will enable a constant electrical output from renewable sources such as wind or solar, when they stop generating power due to the weather changes or night falls.

Safety problems with lithium-metal and lithium-ion batteries can arise when they are charged and discharged, corresponding to electroplate and strip the metal, repeatedly. Over time, the lithium-metal surface becomes rough, which can lead to thermal runaway when the battery literally burns until all the reactants inside are used up. Such problems are avoided in lithium–air batteries because only one of the reactants is contained in the battery and infinite air makes a runaway reaction unlikely. This means that lithium–air batteries are inherently safer than previously developed lithium-metal batteries as well as currently available lithium-ion batteries.

For the lithium batteries, the air cathode is the most serious challenge for eventual development [1,2]. One option is to use nanostructure electrode materials, which are key components in the advancement of future energy-storage technologies due to their high capacity and good cycle ability [6,7]. Nanostructure manganese oxides, such as dendritic clusters, nanocrystals, nanowires, nanotubes, nanobelts and nanoflowers, have been synthesised [8–10]. Among manganese oxides, MnO_2 is of great interest for lithium batteries due to its lower cost, lower toxicity and higher

* Corresponding author. Fax: +44 0191 222 5292.
E-mail address: hua.cheng@ncl.ac.uk (H. Cheng).

0378-7753/$ – see front matter © 2009 Elsevier B.V. All rights reserved.
doi:10.1016/j.jpowsour.2009.09.030

average voltage and its energetic compatibility in a reversible lithium electrochemical system, compared to vanadium-based oxides [11]. Composite electrode materials, such as amorphous manganese oxide coated onto acetylene black, have demonstrated a relatively high discharge-specific capacity [12]. However, there remains the challenge of achieving practical recharge ability for its use as the positive electrode in lithium secondary batteries and better positive electrode materials for lithium–air batteries are highly demanded. Recently, a type of rechargeable oxygen electrode for lithium batteries was reported [3,4]. The oxygen electrode was made by mixing Super S carbon powder, electrolytic manganese dioxide catalysts and Kynar 2801 polymer binder together, to form a porous composite material. In situ mass spectrometry measurements confirmed that oxygen reduction was reversible on such an oxygen electrode, i.e. the Li_2O_2 formed on discharging the oxygen electrode was decomposed to Li and O_2 during charging. Charge/discharge cycling on such an oxygen electrode was also sustainable [4]. An important step to forward the above work is to optimise oxygen electrodes for rechargeable lithium–air batteries.

This work used a different approach by direct loading manganese oxides onto carbon supports, aiming at optimising lithium–air batteries by minimising the amount of catalyst and binder required yet maintaining enhanced energy storage and stability. By applying nano-technology and catalysis methodology, we created a mesoporous carbon-supported metal oxide catalysts, with a different loadings of manganese oxides together with the carbon host by controlling precursors and reaction conditions. The materials were evaluated as the positive electrodes of lithium–air batteries.

2. Experimental

2.1. Catalyst materials

Carbon-supported manganese oxides (MnO_x/C) were synthesised using a redox reaction of manganese sulphate and potassium permanganate in the presence of carbon matrix:

$$2MnO_4^- + 3Mn^{2+} + 2H_2O \rightarrow 5MnO_2 + 4H^+ \quad (1)$$

In practice, a closed glass container with a water jacket containing 150 ml water was heated to 80 °C using a thermal circulating water bath (TE-10A, Techne). Under magnetic stirring, 1.0 g carbon powder was added to the hot water and stirred for 20 min at 80 °C. Then 0.4 g $MnSO_4 \cdot H_2O$ (99%, Sigma) and 1.1 g $KMnO_4$ (99.5%, BDH) were dissolved in 25 ml hot water (80 °C) separately. Both solutions was added to the container drop by drop under magnetic stirring and kept at 80 °C for 1 h. The suspension was filtered and washed several times using distilled water, and then dried at 120 °C overnight. The produced materials were treated at several temperatures but only results obtained using the best catalyst (annealed at 300 °C) and not treated sample are reported in this paper. The material had a catalyst loading around 28 wt% for Mn and 45 wt% for MnO_2. Super P (Timcal), Acetylene (AC, Alfa Aesar) and Norit carbon black (SX, Norit) were used.

Carbon-supported electrolytic manganese dioxide (EMD, Aldrich) materials were formed by directly mixing carbon powder and EMD together.

Transmission electron microscopy (TEM) images were taken using a Philips CM100 transmission electron microscope. The TEM samples were prepared by dispersing carbon-supported manganese oxide materials in anhydrous ethanol with ultra-sonic vibration for 3 min, and then a drop of the supernatant was then transferred onto a standard carbon-covered-copper TEM grid.

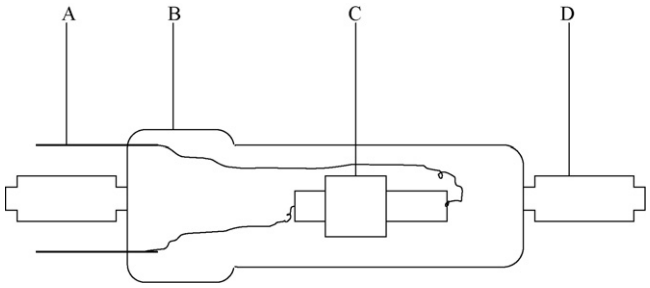

Fig. 1. A schematic of the Li–air battery. A: current collector. B: glass container. C: the Swagelok cell. D: Youngs' tap.

2.2. Batteries and cycle performance test

A Swagelok type battery was used to investigate cycling. It had a stainless steel cylinder plunger to support a Li metal anode (Sigma–Aldrich 265985), together with an aluminium tube to allow oxygen access to back side of cathode. A glass microfibre filter (No. 1825-257, Whatman) separator was used, soaked in 1 M $LiPF_6$ (≥99.99%, Aldrich) in propylene carbonate (Sigma–Aldrich) electrolyte. The cathode was formed by casting a mixture of carbon powder, carbon-supported manganese oxide or EMD and Kynar 2801 binder (Elf Atochem), together with acetone (Aldrich). The cathode is placed onto the separator and a thin open aluminium mesh (Aldrich) is placed on top to act as a current collector. The aluminium plunger is then inserted into the top of the cell and the end cap tightened to hold it in place.

The Swagelok cells were placed into glass containers (Fig. 1). Glass containers consist of sealed vacuum tube with two Youngs' taps for gas flow and two electrical pass through connectors (Tempatron Ltd.). The anode and cathode were connected via crocodile clips to the electrical pass through of the encapsulating glass tubes (Fig. 1). The battery was gastight except for the Al mesh window that exposed the porous cathode to the O_2 atmosphere (1 atm pure oxygen), as shown in Fig. 1.

All processes of assembling and dismantling the batteries were carried out in an argon atmosphere in a glove box (Unilab, MBRAUN, Germany) which provided both water and oxygen levels less than 0.1 ppm. All component parts are washed in distilled water then ethanol (agitating in an ultra-sonic bath) prior to drying at 120 °C

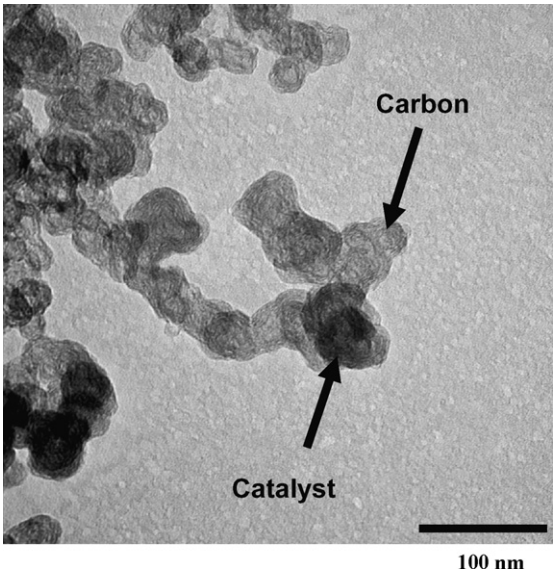

Fig. 2. TEM image of the Norit carbon-supported manganese oxide.

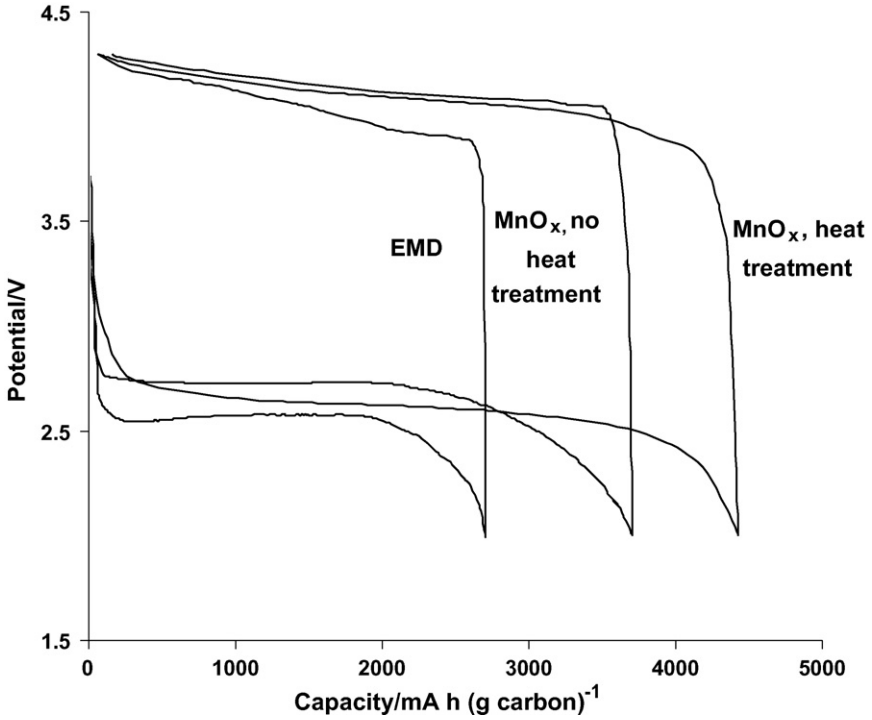

Fig. 3. Voltage–capacity curves on discharge then charge for the Li–air battery with the Norit carbon-supported manganese oxide (heat treated or not treated) or EMD oxygen electrodes at a rate of 70 mA (g carbon)$^{-1}$. The first cycle, which were cycled between 2.0 and 4.3 V in 1 atm of O_2. Capacities are presented as values of per gram of carbon in the electrode.

and transfer to the glove boxes. After cell tubes were removed from the glovebox, they were placed under flowing pure oxygen (BOC) for 1 h.

Battery tests were performed in a temperature controlled oven at 30 °C using a Maccor-4000 battery tester (Maccor). Charge–discharge curves were recorded galvanostatically at a rate of 70 mA (g carbon)$^{-1}$. The batteries were first discharged and then charged between the potential limits of 2.0 V (vs. Li/Li$^+$) for discharge and 4.3 V (vs. Li/Li$^+$) for charge.

3. Results and discussion

3.1. Characterisation

The structure of the carbon-supported manganese oxide was examined with a transmission electron microscope (TEM). As shown in Fig. 2, materials were highly porous; oxides were uniformly distributed on the carbon matrix and were around 20–50 nm in diameter, indicating that the synthesis procedure had effectively produced good nanocatalysts.

3.2. Cycle feature

Fig. 3 (curve "MnO_x, heat treatment") shows the voltage–capacity curves of the carbon-supported manganese oxide oxygen electrode in a rechargeable lithium–oxygen battery. Capacity was measured between 2.0 and 4.3 V vs. Li/Li$^+$. During the discharge process, potentials fell rapidly, after 250 mAh g (carbon)$^{-1}$, to plateau at about 2.7 V, then around 3500 mAh g (carbon)$^{-1}$, decreased continuously to 2.0 V. The discharge potential (2.5–2.7 V) was in good agreement with that reported previously for a similar battery discharged in 1 atm of oxygen [3]. The discharge capacity was about 4150 mAh g (carbon)$^{-1}$.

Such a good performance of the nanomaterials was attributed to their structures which acted as transport pores and ensured rapid insertion and removal of lithium via the following reversible reaction:

$$2Li + O_2 \Leftrightarrow Li_2O_2 \quad (2)$$

The reason for termination of the discharge process was increased polarisation because solid Li_2O_2 were formed and filled the pores [3]. In the charge process, the voltage increased sharply to reach plateau at about 3.9 V and recharging occurred at 3.9–4.3 V.

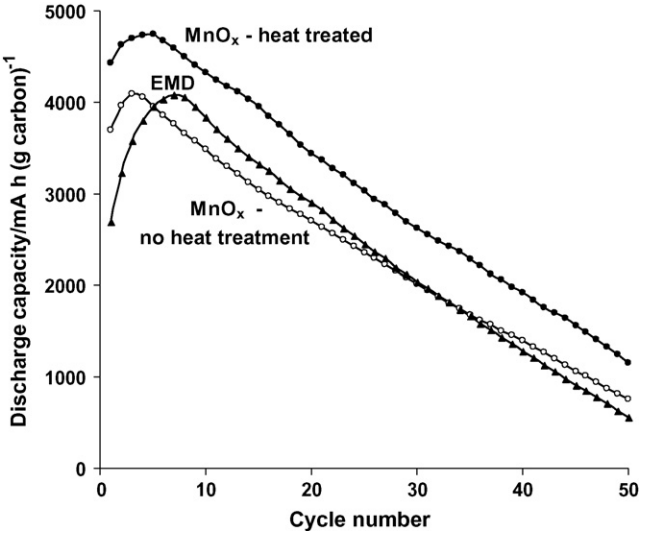

Fig. 4. The relationship between specific capacity and cycle number for the Li–air batteries with the Norit carbon-supported manganese oxide (heat treated or not treated) or EMD oxygen electrodes. Other conditions as in Fig. 3.

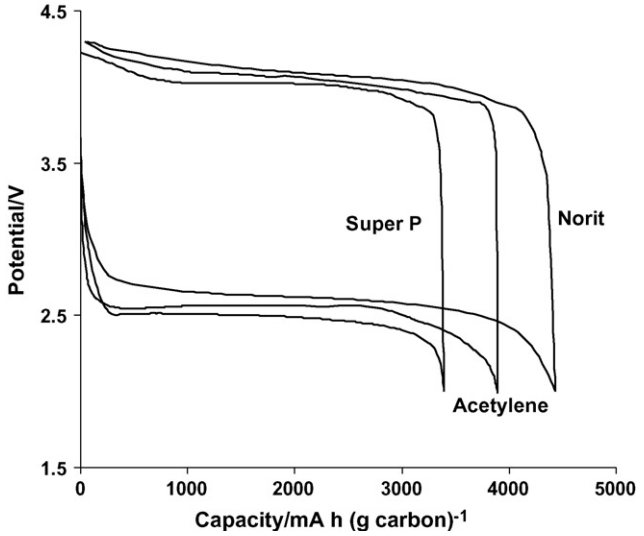

Fig. 5. Voltage–capacity curves on discharge then charge for the Li–air batteries with the Norit, Acetylene or Super P carbon-supported manganese oxide oxygen electrodes. Other conditions as in Fig. 3.

3.3. Effect of catalyst

Fig. 3 also compares cycle performances of rechargeable lithium–oxygen batteries with our manganese oxide catalysts to that with a commercial EMD catalyst, where charge/discharge cycles were carried out at a rate of 70 mAh (g carbon)$^{-1}$. The MnO_x/C catalyst was superior to the commercial EMD, e.g. higher discharge capacity, 4400 cf. 2700 mAh (g carbon)$^{-1}$. This suggests that the synthesis strategy used was effective and the MnO_x/C catalyst had better catalytic activity than the commercial EMD, due to better dispersion and connection between catalysts and the carbon matrix. The cycle performance, as shown in Fig. 4, also proved that the MnO_x/C catalyst (curve "MnO_x-heat treated") was better than EMD (curve "EMD"). Initially, discharge capacities increased and reached maximum values, i.e. 4700 and 4100 mAh (g carbon)$^{-1}$ for the batteries with the MnO_x/C and EMD air electrodes, respectively. After the 50th cycle, the same discharge capacity order remained unchanged; indicating that charge/discharge cycling on the carbon-supported manganese oxide oxygen electrode was sustainable, showing better cycle ability than EMD. The capacity loss of a positive electrode during cycles is a common phenomenon for lithium batteries as a result of the loss and deterioration of the active material and the decrease of the conduction between the active material and the collector [13]. The larger capacity loss of the battery with the EMD catalyst, compared to that with the MnO_x/C catalyst, is understandable because the EMD positive electrode was made by mechanical mixing, so contact areas of catalysts to the carbon support are expected to be smaller than the MnO_x/C electrode which had better contact between carbon and catalysts due to different fabrication procedure.

Heat treatment of carbon-supported manganese oxides affected the battery performance greatly, as shown in Figs. 4 and 5. In general, after annealing at 300 °C, the carbon-supported manganese oxide showed better performance. For example, at the first cycle (Fig. 3), the battery with the heat treated MnO_x/C catalyst displayed higher discharge capacity than that not treated, 4400 cf. 3700 mAh (g carbon)$^{-1}$. The discharge capacity reached about 3450 mAh (g carbon)$^{-1}$ after 20 cycles, which was more than 30% increase, compared to the non-treatment counterpart (Fig. 4, curves "MnO_x-heat treated" vs. "MnO_x-not treated"). At the 50th cycle, the increment was more than 50% (Fig. 4, curves "MnO_x-heat treated" vs. "MnO_x-not treated"). This means that the heat treatment increased the catalyst capacity via removed impurities, increased porosity, etc.

3.4. Effect of carbon

Fig. 5 shows the effect of carbon type on the performance of rechargeable lithium–oxygen batteries with Super P, Acetylene or Norit carbon black-supported manganese oxide catalysts. The contributions to capacities were from both catalyst and carbon and, because the same MnO_x catalyst was used, the difference in capacity was due to different carbon supports. Based on discharge capacity data, the performance order was established as: Norit (4400 mAh (g carbon)$^{-1}$) > acetylene (3900 mAh (g carbon)$^{-1}$) > Super P (3400 mAh (g carbon)$^{-1}$), sug-

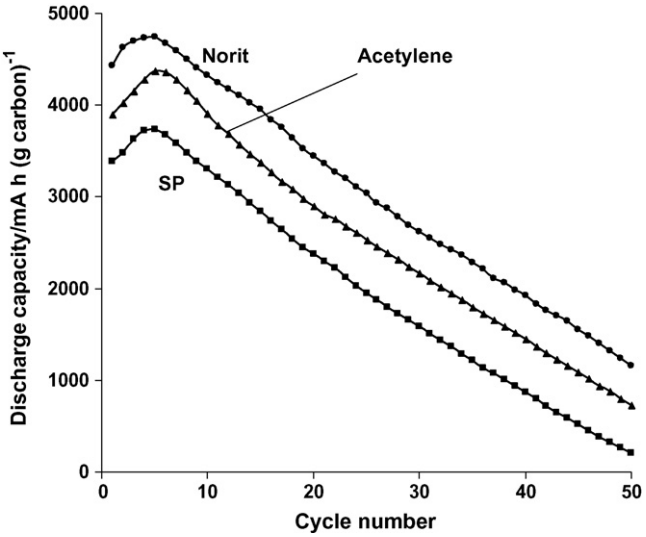

Fig. 6. Variation of discharge capacity with cycle number for the Li–air batteries with the Norit, Acetylene or Super P carbon-supported manganese oxide oxygen electrodes. Other conditions as in Fig. 3.

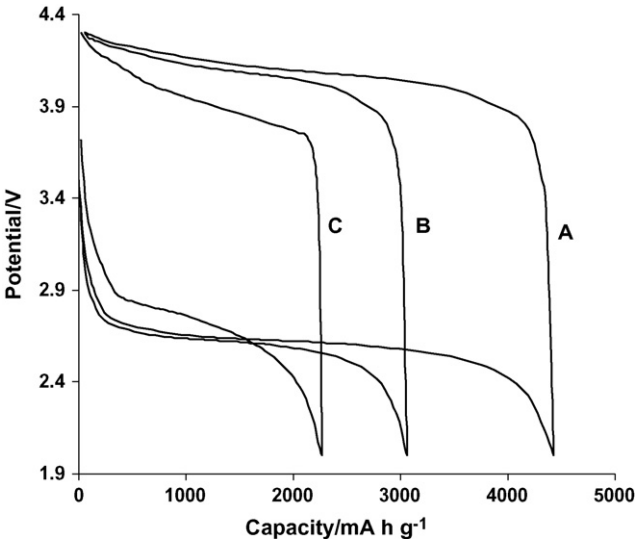

Fig. 7. Variation of potential with state of charge for the Li–air batteries with the Norit carbon black-supported manganese oxide electrodes. Electrode compositions:

	Sample		
	A	B	C
MnO_x (wt%)	20	15	5
Norit carbon (wt%)	10	15	25

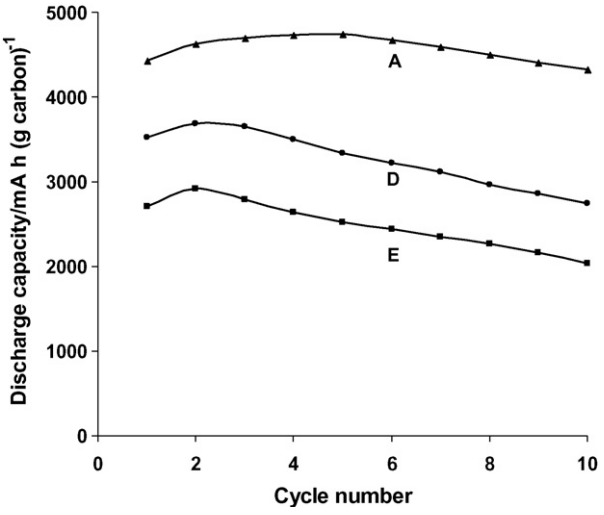

Fig. 8. The relationship between specific capacity and cycle number the Li–air batteries with the carbon-supported manganese oxide oxygen electrode. Electrode compositions:

	Sample		
	A	D	E
Kynar (wt%)	15	20	10
Propylene carbonate (wt%)	55	50	60
MnO_x (wt%)	20	20	20
Norit carbon (wt%)	10	10	10

gesting that Norit carbon black was a better support than others under rechargeable lithium–oxygen batteries conditions. This may partly attributed to their different surface areas, i.e. 800, 75 and 62 $m^2\,g^{-1}$ for Norit [14], Acetylene [15] and Super P carbon black [16] 1, respectively. The difference in surface area led to differences in catalyst dispersion and contact areas of catalyst to carbon support and to different catalytic activities.

Fig. 6 shows the cycle performance for the different carbon-supported catalysts, which confirmed the above order. For instance, at the 50th cycle, discharge capacities were 1150, 730 and 200 mAh (g carbon)$^{-1}$ for Norit, Acetylene and Super P carbon black, respectively.

3.5. Effect of electrode composition

The effect of changing the ratio of catalyst to carbon (2:1, 1:1 and 1:5) on the battery performance is shown in Fig. 7. A catalyst to carbon ratio of 20 to 10 in weight showed the highest discharge capacity, i.e. 4400 mAh (g carbon)$^{-1}$ vs. 3050 and 2260 mAh (g carbon)$^{-1}$ for other ratios. This indicates that the electrode with catalyst to carbon ratio of approximately 2:1 had a suitable structure for the battery.

Fig. 8 shows the effect of Kynar binder on the battery performance, with a fixed catalyst and carbon weights, i.e. 20 wt% catalysts and 10 wt% carbons. The electrode with 15 wt% Kynar showed higher discharge capacities than the other electrodes, e.g. at the 5th cycle, 4750 mAh (g carbon)$^{-1}$ against 3300 and 2500 mAh (g carbon)$^{-1}$ for other electrodes. The data suggested that, at this composition, there was a better contact between active catalysts and carbon supports. Therefore, the addition of 15 wt% represents a good balance between the requirement for good adhesion, acceptable conductivity and the access of oxygen.

4. Conclusions

Carbon-supported manganese oxide catalysts were successfully fabricated and used as positive electrodes for rechargeable lithium–oxygen batteries. High discharge capacities up to 4750 mAh (g carbon)$^{-1}$ were achieved, which was higher than that with a commercial EMD catalyst. Norit carbon black showed the best performance of carbons investigated. Performance was influenced by the electrode composition in terms of catalyst to carbon ratio and Kynar binder. The cycling ability of the battery with carbon-supported manganese oxide was superior to that with commercial electrolytic manganese dioxide electrodes.

Acknowledgements

The authors thank the EPSRC for funding and an EPSRC/HEFCE Joint Infrastructure Fund award (No. JIF4NESCEQ) for research facilities. TEM measurements provided by the Electron Microscopy Research Services at Newcastle University.

References

[1] M. Armand, J.-M. Tarascon, Nature 451 (2008) 652.
[2] P.G. Bruce, Solid State Ionics 179 (2008) 752.
[3] A. Debart, J.L. Bao, G. Armstrong, P.G. Bruce, J. Power Sources 174 (2007) 1177.
[4] T. Ogasawara, A. Debart, M. Holzapfel, P. Novak, P.G. Bruce, J. Am. Chem. Soc. 128 (2006) 1390.
[5] K.M. Abraham, Z. Jiang, J. Electrochem. Soc. 143 (1996) 1.
[6] H. Baughman, A.A. Zakhidov, W.A. de Heer, Science 297 (2002) 787.
[7] F. Raimondi, G.G. Scherer, R. Kotz, A. Wokaun, Angew. Chem. Int. Ed. 44 (2005) 2190.
[8] M.S. Wu, P.J. Chiang, J.T. Lee, J.C. Lin, J. Phys. Chem. B 109 (2005) 23279.
[9] E.S. Toberer, T.D. Schladt, R. Seshadri, J. Am. Chem. Soc. 128 (2006) 1462.
[10] H. Zhang, G.P. Cao, Y.S. Yang, Z.N. Gu, J. Electrochem. Soc. 155 (2008) K19.
[11] M.M. Thackeray, W.I.F. David, P.G. Bruce, J.B. Goodenough, Mater. Res. Bull. 18 (1983) 461.
[12] H. Kawaoka, M. Hibino, H.S. Zhou, I. Honma, J. Power Sources 125 (2004) 85.
[13] M.-S. Wu, P.-C. Julia Chiang, J.-T. Lee, J.-C. Lin, J. Phys. Chem. B 109 (2005) 23279.
[14] Company catalogue at http://www.norit-americas.com.
[15] Company catalogue at http://www.alfa.com.
[16] Company catalogue at http://www.timcal.com.